Structure–Activity Relationships for Xenobiotic Transport Substrates and Inhibitory Ligands of P-glycoprotein

Lisa J. Bain, James B. McLachlan, and Gerald A. LeBlanc

Department of Toxicology, North Carolina State University, Raleigh, NC 27695 USA

The multixenobiotic resistance phenotype is characterized by the reduced accumulation of xenobiotics by cells or organisms due to increased efflux of the compounds by P-glycoprotein (P-gp) or related transporters. An extensive xenobiotic database, consisting primarily of pesticides, was utilized in this study to identify molecular characteristics that render a xenobiotic susceptible to transport by or inhibition of P-gp. Transport substrates were differentiated by several molecular size/shape parameters, lipophilicity, and hydrogen bonding potential. Electrostatic features differentiated inhibitory ligands from compounds not catagorized as transport substrates and that did not interact with P-gp. A two-tiered system was developed using the derived structure–activity relationships to identify P-gp transport substrates and inhibitory ligands. Prediction accuracy of the approach was 82%. We then validated the system using six additional pesticides of which two were predicted to be P-gp inhibitors and four were predicted to be noninteractors, based upon the structure–activity analyses. Experimental determinations using cells transfected with the human *MDR1* gene demonstrated that five of the six pesticides were properly catagorized by the structure–activity analyses (83% accuracy). Finally, structure–activity analyses revealed that among P-gp inhibitors, relative inhibitory potency can be predicted based upon the surface area or volume of the compound. These results demonstrate that P-gp transport substrates and inhibitory ligands can be distinguished using molecular characteristics. Molecular characteristics of transport substrates suggest that P-gp may function in the elimination of hydroxylated metabolites of xenobiotics. *Key words*: multidrug resistance, multixenobiotic resistance, pesticides, P-glycoprotein, structure–activity relationships. *Environ Health Perspect* 105:812–818 (1997)

http://ehis.niehs.nih.gov

P-glycoprotein (P-gp) is a 170 kDa protein, encoded by the human *MDR1* gene, which has been shown to efflux a wide variety of drugs such as the chemotherapeutic agents doxorubicin, vincristine, and vinblastine (*1*). P-gp in humans is located on the secretory surfaces of organs of elimination, such as the brush border of the renal proximal tubules, the canalicular membrane of hepatocytes, and the apical surface of mucosal cells in the small and large intestines (*2*). This tissue localization and direct experimental evidence (*3*) indicates that P-gp plays a role in eliminating xenobiotics from the whole organism. P-gp is also localized in hormone-producing and hormone-responsive organs such as the adrenal gland, the testes, and the placenta (*2*). Steroid hormones such as cortisol (*4*), corticosterone (*5*), and aldosterone (*6*) have been shown to be transport substrates for P-gp.

The involvement of P-gp in pesticide toxicity was shown with the anthelmintic agent ivermectin. *Mdr1a* gene-knockout mice treated with the neurotoxic pesticide ivermectin demonstrated increased sensitivity to this pesticide and increased accumulation of this pesticide in the brain as compared to control mice (*7*). When C57BL/6 mice were cotreated with ivermectin and the P-gp inhibitors SDZ PSC833 or SDZ 280-446, the mice were hypersensitive to the neurotoxic effects of ivermectin compared to treatment with ivermectin alone (*8*). Additionally, rats treated with the pesticide chlorpyrifos showed increased P-gp protein levels in the bile duct, adrenal gland, stomach, jejunum, and kidney proximal tubules (*9*). Thus, P-gp appears to play a role in both the efflux of chemicals from cells and the elimination of chemicals from the body.

Many compounds have been shown to inhibit P-gp function, and the use of P-gp inhibitors has received significant attention as a possible means of enhancing the efficacy of drugs transported by this protein by decreasing their rate of efflux (*10*). Holfsli and Nissen-Meyer (*11*) observed that 73% of 26 drugs assessed inhibited P-gp *in vitro*. Studies in our laboratory have shown that many pesticides can inhibit P-gp function (*12*). Although the structures of P-gp inhibitors differ significantly, common characteristics include a molecular mass greater than 300 (*13,14*) and lipophilicity (*11*). Additional characteristics associated with some P-gp inhibitors include amphipathic properties (*15*) and a positive charge at physiological pH (*1,10,15*). Molecular characteristics of transport substrates of P-gp are less well understood; however, P-gp inhibitors have been typically assumed to competitively inhibit transport substrates (*11,16*), suggesting that inhibitory ligands and transport substrates share similar molecular characteristics.

In a previous study, we assessed the ability of 38 pesticides to inhibit P-gp function (*12*). Based upon these results, we concluded that chemicals with the greatest potential to inhibit P-gp contained a cyclic structure within the molecule, a molecular mass of 391–490 Da, and a log K_{ow} of 3.6–4.5. Seven of the inhibitory pesticides were evaluated for susceptibility to transport by P-gp, but only one of the pesticides was transported by P-gp. These results demonstrated that many pesticides are capable of inhibiting P-gp function; however, inhibition does not imply that the pesticide is transported by P-gp. Thus, transport substrates of P-gp may have significantly different molecular characteristics than inhibitory ligands.

In the present study, we significantly refined our structure–activity analysis of P-gp inhibition by pesticides. In addition, the structural attributes of P-gp inhibitors were compared to those of known P-gp substrates in order to define characteristics that dictate whether a chemical will either inhibit or be transported by P-gp. Six new pesticides were then subjected to the structure–activity analyses in order to predict the level of interaction with P-gp; these predictions were then validated experimentally.

Materials and Methods

Structure–activity analyses. Molecular attributes used in the structure-activity analyses were calculated using Molecular Modeling Pro software (NorGwyn Montgomery Software, Inc., North Wales, PA). Known P-gp transport substrates and pesticides previously shown to inhibit P-gp (*12*) were selected for analysis. In addition, 15 pesticides that had previously been shown not to interact with P-gp (*12*) were randomly selected to provide an approximately equal number of transport substrates, inhibitory ligands, and noninteracting compounds. These compounds were analyzed for the following molecular descriptors as described (with citations) in the software manual:

- Molecular weight was calculated as the sum of the individual weights of the atoms comprising the molecule (values are exact)

Address correspondence to G.A. LeBlanc, Department of Toxicology, North Carolina State University, Box 7633, Raleigh, NC 27695 USA.

This work was supported by NIEHS grant PO1 ES-00044.

Received 6 March 1997; accepted 22 April 1997.

- Surface area was calculated as the surface area of spheres of Van der Waals radii minus overlaps (values are accurate)
- Volume was calculated as the volume of spheres of Van der Waals Radii minus overlaps (values for volume are accurate)
- Kappa shape represented Kier's index of shape (values are exact)
- Connectivity 0,1,2,3 indices were derived from Randic's graph theory. Values of connectivity provide clues to the shape and size of molecules (values are exact)
- Dipole moment was calculated using the DelRe method of calculating partial charge strength and location (dipole moment values are affected by molecular conformation but are reasonably accurate)
- Valence indices 0,1,2,3 provided measures of various electrostatic features of the molecule (values are accurate)
- Percent hydrophilic surface was calculated using an algorithm that determines which components of the molecule are hydrophilic. Hydrophilic surface was divided by total surface area (as defined above) × 100 (values are reasonably accurate)
- The hydrophilic–lipophilic balance was obtained by dividing the molecular weight of the water soluble portions of the molecule by the total molecular weight × 20 (values are accurate)
- Dispersion (Hansen 3-D parameter) measured the repulsive forces between molecules (values are moderately to very accurate)
- The log K_{ow} (log octanol:water partition coefficient) was calculated by the modified Hansch fragment addition method. Values are accurate for small ortanic molecules; accuracy decreases as molecular mass and complexity increases
- Solubility was calculated as the square root of the sum of squares of dispersion, polarity, and H bonding (values are fairly accurate)
- Polarity (Hansen 3-D parameter) measured the localization of positive and negative charges associated with a molecule (values are moderately to very accurate)
- Hydrogen bonding (Hansen 3-D parameter) measured the tendency of a molecule to form hydrogen bonds (accuracy varies among molecules)
- Aromatic structures indicates the sum of 6-membered aromatic rings in the molecule (values are exact)
- Total cyclic structures represents the sum of closed chain (both aromatic and nonaromatic) features (values are exact).

Compounds were grouped into three classes: transport substrates, inhibitory ligands, or noninteractors. For each molecular descriptor, means and standard deviations were calculated within each class, and significant differences between classes was evaluated by the Student's *t*-test.

Pesticides. Azinphos-ethyl, coumaphos, fluazifop *p*-butyl, phosalone, and triforine were purchased from Chem Service (West Chester, PA). Dialifos was purchased from Crescent Chemical Company (Hauppauge, NY). All pesticides were at least 98% pure.

Cell lines. The parental murine melanoma cell line B16/F10 was transfected with the human *MDR1* gene by a replication-defective amphitrophic retrovirus to generate the P-gp-overexpressing B16/hMDR1 cell line. The cells were cultured in RPMI 1640 medium supplemented with 10% fetal bovine serum (Gibco BRL, Gaithersburg, MD) at 37°C in a humidified atmosphere of 5% CO_2/95% air. The expression of P-gp, as well as the characterization of the multixenobiotic resistance phenotype (MXR), in these cells has been described previously (*12,14*). The MXR phenotype of the B16/hMDR1 cells was maintained by intermittently culturing the cells in 6 µM vinblastine (Sigma Chemical Company, St. Louis, MO).

Transport of pesticides by P-glycoprotein. B16/F10 and B16/hMDR1 cells were plated in 35-mm petri dishes at a density of 0.8–1.0 × 10^6 cells/plate and were allowed to attach overnight. The next morning, the medium was aspirated off and replaced with medium containing 100 µM of the pesticide of interest. Plates were incubated at 37°C for 4 hr after which the medium was removed and the cells were washed twice with ice-cold phosphate-buffered saline (PBS) and were overlaid with fresh medium to allow for efflux. After defined efflux periods, the medium was aspirated off and the cells were washed again with ice-cold PBS. The cells were scraped into PBS and lysed by pulse sonication, and the suspension was extracted twice with ethyl acetate. Extraction efficiencies of the six pesticides were 81–98%. The extract was evaporated under nitrogen and the residue dissolved in HPLC mobile phase. The amount of pesticide remaining in the cells was detected by HPLC on a Waters LC Module 1 Plus (Waters, Milford, MA) equipped with a reverse-phase Nova-Pak C_{18} column (3.9 × 150 mm, 4 µm pore size). The mobile phase for phosalone was 80% methanol/20% water at 1 ml/min with detection at 235 nm (*17*). The mobile phase for coumaphos was 85% acetonitrile/15% water at 2 ml/min with detection at 313 nm (*18*). The mobile phase for azinphos-ethyl was 80% methanol/20% water at 1 ml/min with detection at 220 nm. The mobile phase for dialifos was 67% acetonitrile/33% water at 1.4 ml/min with detection at 225 nm. The mobile phase for fluazifop *p*-butyl was 71% acetonitrile/29% water acidified to pH 3.0 with phosphoric acid at 1 ml/min and detection at 270 nm (*19*). The mobile phase for triforine was 80% methanol/20% water at 1 ml/min with detection at 202 nm. Results from three replicates per cell line are presented for at least five time points during the efflux period. Each data point represents the percentage of pesticide remaining in the cells relative to the amount present in the cells at the beginning of the efflux period.

The efflux of two known P-gp substrates, doxorubicin and vincristine, were assessed in the two cell lines as positive controls. Doxorubicin was incubated with the cells at a concentration of 50 µM. To extract the doxorubicin associated with the cells, they were suspended in 1 ml PBS containing 100 µl of 0.1 M Tris buffer, pH 8.4, and extracted into 5 ml chloroform. The mobile phase for doxorubicin consisted of 52% water/48% acetonitrile, 10 mM SDS, 20 mM phosphoric acid at a flow rate of 1.5 ml/min with detection at 233 nm (*20*). Cells were incubated in 7 µM vincristine and were extracted from the cells into 5 ml chloroform. The mobile phase for vincristine detection was 60% acetonitrile/40% 25 mM phosphate buffer, pH 2.7, adjusted with phosphoric acid, containing 0.25 g/l SDS at a flow rate of 0.9 ml/min with detection at 238 nm (*21*).

Inhibition of P-glycoprotein by pesticides. B16/F10 and B16/hMDR1 cells (0.2–1.0 × 10^6 cells/assay) were placed in microfuge tubes containing 50 µM doxorubicin (Pharmacia, Columbus, OH) in RPMI 1640 medium and either various concentrations of the pesticide or 10 µM verapamil (Sigma), the positive control. Cells were incubated at 37°C for 4 hr before being pelleted by centrifugation and washed with ice-cold PBS. The pellet was resuspended and the cells washed again before extraction solution (0.6 N HCl in 50% water/50% ethanol) was added to each tube. The pellet was then vortexed and the tubes were refrigerated overnight. The amount of doxorubicin associated with the cells was measured fluorimetrically at 470 nm excitation and 585 nm emission (*22*). The results are presented for at least six concentrations of pesticide using three replicates per cell line. The effective concentration (EC_{50}) of the pesticide required to increase the level of doxorubicin associated with the B16/hMDR1 cells to half of that obtained with cells containing 10 µM verapamil (maximum inhibition) was calculated by Spearman-Karber regression analysis (*23*).

Results

Structure–activity analysis of P-glycoprotein transport substrates and inhibitory ligands. Previous work in our laboratory has shown that the optimal characteristics for a pesticide to interact with P-gp are at least one cyclic structure, a molecular weight of 391–490 Da, and a log K_{ow} 3.6–4.5. While those character-

istics provide optimal binding to P-gp, only one of seven pesticides that show evidence of binding to P-gp was actually transported by this protein. Forty-four compounds were analyzed in the present study, including 11 transport ligands, 18 inhibitors, and 15 noninteractors (Table 1). Compounds were evaluated for various molecular attributes including size/shape parameters (molecular weight, surface area, volume, kappa shape, connectivity indices 0–3), electrostatic parameters (dipole moment, valence indices 0–3), solubility parameters (log K_{ow}, solubility, polarity, percent hydrophilic surface, hydrophilic–lipophilic balance), hydrogen bonding potential, cyclic components, and others (Table 2).

Predominant molecular characteristics that significantly differ among the compound classes are size/shape, with molecular weight and cyclic structures being the most informative attributes; solubility, with log K_{ow} being the most informative attribute; hydrogen bonding potential; and electrostatic parameters, with dipole moment being most informative. Based upon these analyses, criteria were developed for the differentiation of transport substrates, inhibitory ligands, and noninteracting compounds using a two tiered approach. The first tier was used to differentiate transport substrates from inhibitory ligands and noninteracting compounds. Compounds were classified as transport substrates if they met all of the following tier 1 criteria: 1) the compound had at least one ≥6-membered cyclic structure; 2) the molecular weight was >399; 3) the log K_{ow} was <2; and 4) hydrogen bonding potential was >8.

Remaining compounds were classified as inhibitory ligands if they met all of the following tier 2 criteria: 1) the compound had at least one ≥6-membered cyclic structure; 2) the molecular weight was >247; and 3) the dipole moment was ≥3.3.

Compounds that met neither the tier 1 nor tier 2 criteria were catagorized as noninteracting compounds. Using these criteria, transport substrates, inhibitory ligands, and noninteracting compounds were detected with 82%, 72%, and 89% accuracy, respectively.

In an attempt to validate these criteria, six previously untested pesticides were subjected to the two tier structure–activity analysis (Table 3). None of the pesticides were predicted to be transport substrates based upon molecular weight, log K_{ow}, or hydrogen bonding considerations. Coumaphos and phosalone were predicted to be P-gp inhibitors while azinphos-ethyl, dialifos, fluazifop *p*-butyl, and triforine were predicted to be noninteractors. These catagorizations were predicated by differences in dipole moments of the pesticides.

Table 1. Compounds used in structure–activity analyses

Class/compound	Reference
Transport substrate	
Actinomycin D	(1,10)
Doxorubicin	(1,10)
Daunomycin	(1,10)
Vincristine	(1,10)
Vinblastine	(1,10)
Colchicine	(1,10)
Taxol	(1,10)
Endosulfan	(12)
Cyclosporin A	(1,10)
Etoposide	(1,10)
Hydroxyrubicin	(1,10)
Inhibitory ligand	
Chlordecone	(12)
Verapamil	(24)
Nicardipine	(24)
Chlorthion	(12)
Phenamiphos	(12)
Tetrachlorohydroquinone	(12)
Parathion	(12)
Chlorpyrifos	(12)
Fluvalinate	(12)
Permethrin	(12)
Dicapthon	(12)
Heptachlor	(12)
Heptachlor epoxide	(12)
Diltiazim	(24)
Clomipramine	(24)
Hydramethylnon	(12)
Ivermectin	(12)
Clotrimazole	(12)
Noninteractor	
Dieldrin	(12)
Mirex	(12)
Aldicarb	(12)
Phosmet	(12)
Methoxychlor	(12)
Aldoxycarb	(12)
Vinclozolin	(12)
Mevinphos	(12)
Lindane	(12)
Atrazine	(12)
Paraquat	(12)
Carbaryl	(12)
Aminocarb	(12)
Leptophos	(12)
Propiconazole	(12)

Table 2. Structure–activity relationships among noninteractors, inhibitors, and transport substrates of P-glycoprotein

Parameter	Noninteractors (mean ± SD)	Ratio[a]	Inhibitors (mean ± SD)	Ratio	Transporters (mean ± SD)	Ratio
Molecular weight	290.32 ± 102.49[b,c]	1	407.88 ± 147.17[c,d]	1.40	723.49 ± 295.59[b,d]	2.49
Surface area	17.04 ± 3.11[b,c]	1	25.19 ± 12.23[c,d]	1.48	49.61 ± 25.40[b,d]	2.91
Volume	133.38 ± 28.91[b,c]	1	199.36 ± 94.10[c,d]	1.49	388.97 ± 185.58[b,d]	2.92
Kappa shape	5.35 ± 1.54[b,c]	1	8.87 ± 5.18[c,d]	1.66	16.94 ± 10.55[b,d]	3.12
Connectivity 0	23.88 ± 4.43[b,c]	1	38.52 ± 25.84[c,d]	1.61	83.86 ± 47.16[b,d]	3.51
Connectivity 1	7.78 ± 1.70[b,c]	1	11.69 ± 6.33[c,d]	1.50	24.11 ± 10.37[b,d]	3.10
Connectivity 2	7.48 ± 2.16[b,c]	1	11.45 ± 5.37[c,d]	1.53	23.06 ± 9.89[b,d]	3.08
Connectivity 3	6.40 ± 3.06[b,c]	1	9.61 ± 4.76[c,d]	1.50	20.36 ± 7.83[b,d]	3.19
Dipole moment	3.02 ± 1.68[b,c]	1	4.88 ± 2.54[c,d]	1.61	7.94 ± 3.33[b,d]	2.63
Valence index 0	22.64 ± 3.78[b,c]	1	35.96 ± 24.27[c,d]	1.59	76.81 ± 44.49[b,d]	3.39
Valence index 1	6.14 ± 1.94[b,c]	1	9.22 ± 4.28[c,d]	1.50	17.48 ± 7.90[b,d]	2.85
Valence index 2	5.52 ± 2.95[c]	1	7.75 ± 3.79[c]	1.40	14.85 ± 6.67[b,d]	2.69
Valence index 3	4.55 ± 4.17[c]	1	6.11 ± 3.84[c]	1.34	11.33 ± 4.41[b,d]	2.49
Percent hydrophilic surface	71.76 ± 21.11	1	61.96 ± 31.26	0.86	64.51 ± 16.83	0.90
Hydrophilic-lipophilic balance	16.04 ± 3.66	1	14.18 ± 5.63	0.88	15.79 ± 2.52	0.98
Dispersion	20.01 ± 2.63	1	19.57 ± 4.64	0.98	19.42 ± 2.15	0.97
Log K_{ow}	2.88 ± 2.70[c]	1	4.35 ± 1.94[c]	1.51	-0.34 ± 3.35[b,d]	0.12
Solubility	22.87 ± 2.80[c]	1	21.98 ± 5.09[c]	0.96	25.59 ± 3.35[b,d]	1.12
Polarity	7.45 ± 2.59[b]	1	5.35 ± 2.55[c,d]	0.72	8.00 ± 3.03[b]	1.07
Hydrogen bonding	7.18 ± 3.07[c]	1	7.73 ± 3.25[c]	1.08	14.04 ± 3.98[b,d]	1.96
Aromatic structures	1.00 ± 0.94[c]	1	1.29 ± 0.90[c]	1.29	1.55 ± 0.93[b,d]	1.55
Total cyclic structures	1.21 ± 0.85[b,c]	1	1.90 ± 1.18[c,d]	1.57	4.27 ± 1.56[b,d]	3.53

SD, standard deviation.
[a]Ratios are the mean value for that parameter divided by the mean value for the noninteractors.
[b]Significantly different from inhibitors by the Student's *t*-test ($p<0.05$).
[c]Significantly different from transporters by the Student's *t*-test ($p<0.05$).
[d]Significantly different from noninteractors by the Student's *t*-test ($p<0.05$).

Table 3. Molecular parameters used in the structure–activity analyses of pesticides

Parameter	Azinphos-ethyl	Coumaphos	Dialifos	Fluazifop *p*-butyl	Phosalone	Triforine
Molecular weight	345.38	362.77	393.85	383.38	367.81	434.96
Total cyclic structures	2	2	1	2	1	1
Log K_{ow}	4.43	9.84	5.51	6.44	7.99	2.70
Hydrogen bonding	6.91	2.43	6.05	5.69	6.62	10.27
Dipole moment	1.47	7.67	3.29	2.65	4.91	0.70

Transport of pesticides by P-glycoprotein. The susceptibility of the six pesticides, in addition to the known P-gp substrates doxorubicin and vincristine, to P-gp-mediated transport then was determined experimentally. B16/F10 and B16/hMDR1 cells were incubated with each potential substrate for 4 hr; the cells were then washed and allowed to efflux the accumulated compound into clean medium. The amount of potential substrate remaining in the cells at various times during efflux was measured by HPLC. The known P-gp substrates doxorubicin and vincristine were eliminated from the P-gp-expressing B16/hMDR1 cells at a significantly greater rate than from the parental B16/F10 cells (Figs. 1 A, B). In contrast, the six pesticides were eliminated from both cell lines at comparable rates (Figs. 1 C–H). Consistent with the structure–activity predictions, the six pesticides were not P-gp transport substrates.

Inhibition of P-glycoprotein by pesticides. The six pesticides were then evaluated experimentally to identify inhibitors of P-gp. Azinphos-ethyl, coumaphos, and phosalone completely inhibited the P-gp-mediated efflux of doxorubicin as indicated by the increased accumulation of doxorubicin in the B16/hMDR-1 cells (Fig. 2). EC_{50} values were calculated to determine the relative potency of each of these pesticides at inhibiting the P-gp-mediated doxorubicin efflux (Table 4). None of these pesticides were nearly as potent as verapamil (EC_{50} = 3.2 μM), but were within the range of EC_{50} values measured previously for pesticides (*12*). Dialifos, fluazifop *p*-butyl, and triforine had no effect on P-gp function at the highest concentrations tested and were therefore considered to be noninteracting compounds. Structure–activity analyses accurately predicted the interactions of five of the six pesticides (83%). Azinphos-ethyl was shown experimentally to inhibit P-gp, but was predicted to be a noninteractor. Interestingly, azinphos-ethyl was the least potent among the three inhibitory pesticides.

Predicting potency of inhibitory ligands towards P-glycoprotein. This and previous studies (*12*) have shown that the potency with which some xenobiotics inhibit P-gp function varies widely. Therefore, relationships among molecular characteristics and potency of P-gp inhibitors were examined using the inhibitors chlorpyrifos, clotrimazole, dicapthon, hydramethylnon, parathion, and verapamil for which we had previously measured EC_{50} values (*12*). Both molecular surface area (r = 0.93) and volume (r = 0.97) were highly correlated (p = 0.01) to EC_{50} values (Fig. 3). As either the surface area or volume of the molecule increased, the potency of the pesticide to inhibit P-gp also

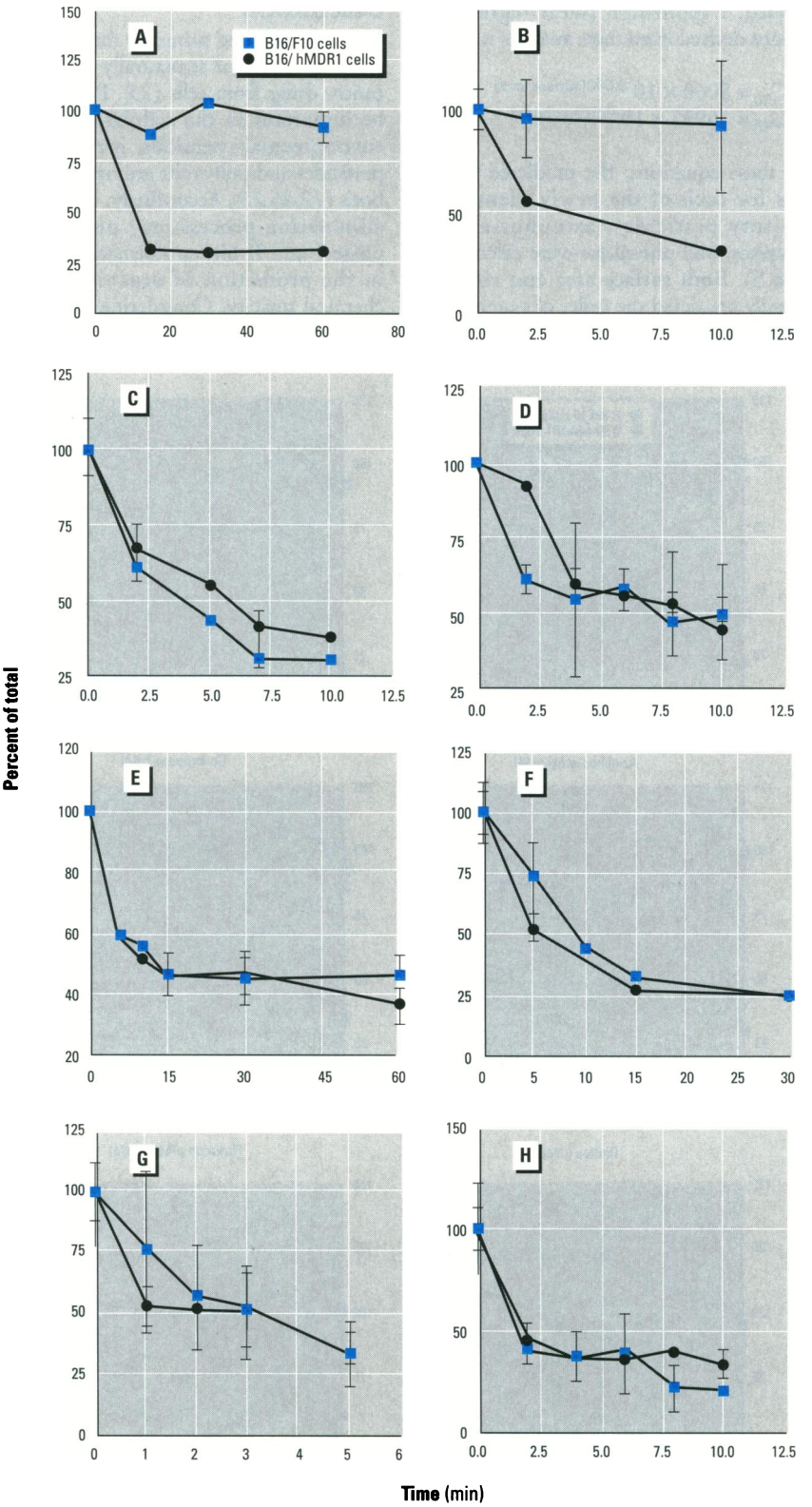

Figure 1. Efflux of pesticides from B16 cells. B16/F10 cells and B16/hMDR1 cells were incubated in (A) 50 μM doxorubicin; (B) 7 μM vincristine; (C) 100 μM phosalone; (D) 100 μM dialifos; (E) 100 μM azinphos-ethyl; (F) 100 μM coumaphos; (G) 100 μM fluazifop *p*-butyl; and (H) 100 μM triforine for 4 hr and allowed to depurate the accumulated pesticide (as described in Materials and Methods). The amount of pesticide remaining in the cells was analyzed by HPLC and is presented as percentage of the initial concentration of pesticide in the cells at the start of the depuration phase. Values are the mean ± standard deviation of three replicates for each time point.

increased. Exponential linear regression equations derived from these analyses were

$$EC_{50} = 8060 \times 10^{-0.098(\text{surface area})} \quad (1)$$
$$EC_{50} = 10937 \times 10^{-0.013(\text{volume})} \quad (2)$$

From these equations, the predicted EC_{50} values for each of the newly identified inhibitory pesticides, azinphos-ethyl, coumaphos, and phosalone were calculated (Table 5). Both surface area and volume accurately predicted the order of potency of the pesticides and predicted the actual EC_{50} values within a factor of 2.

Discussion

P-gp is recognized primarily for its ability to efflux a variety of structurally diverse anticancer drugs from cells (*25*). P-gp may also be important in the cellular clearance of environmental chemicals, including some pesticides and polycyclic aromatic hydrocarbons (*12,26,27*). Accordingly, this phase III elimination process may prove to rival phase I and II biotransformation processes in the protection of organisms against chemical toxicity. Considering the diversity of compounds to which organisms are exposed via food, water, and environment, an understanding of the structural attributes that render a compound susceptible to elimination by P-gp would greatly facilitate the characterization of the role of P-gp in protecting against toxicant insult.

Results from the present analyses indicate that size, shape, solubility, and hydrogen-bonding characteristics are all important determinants of chemical transport by P-gp.

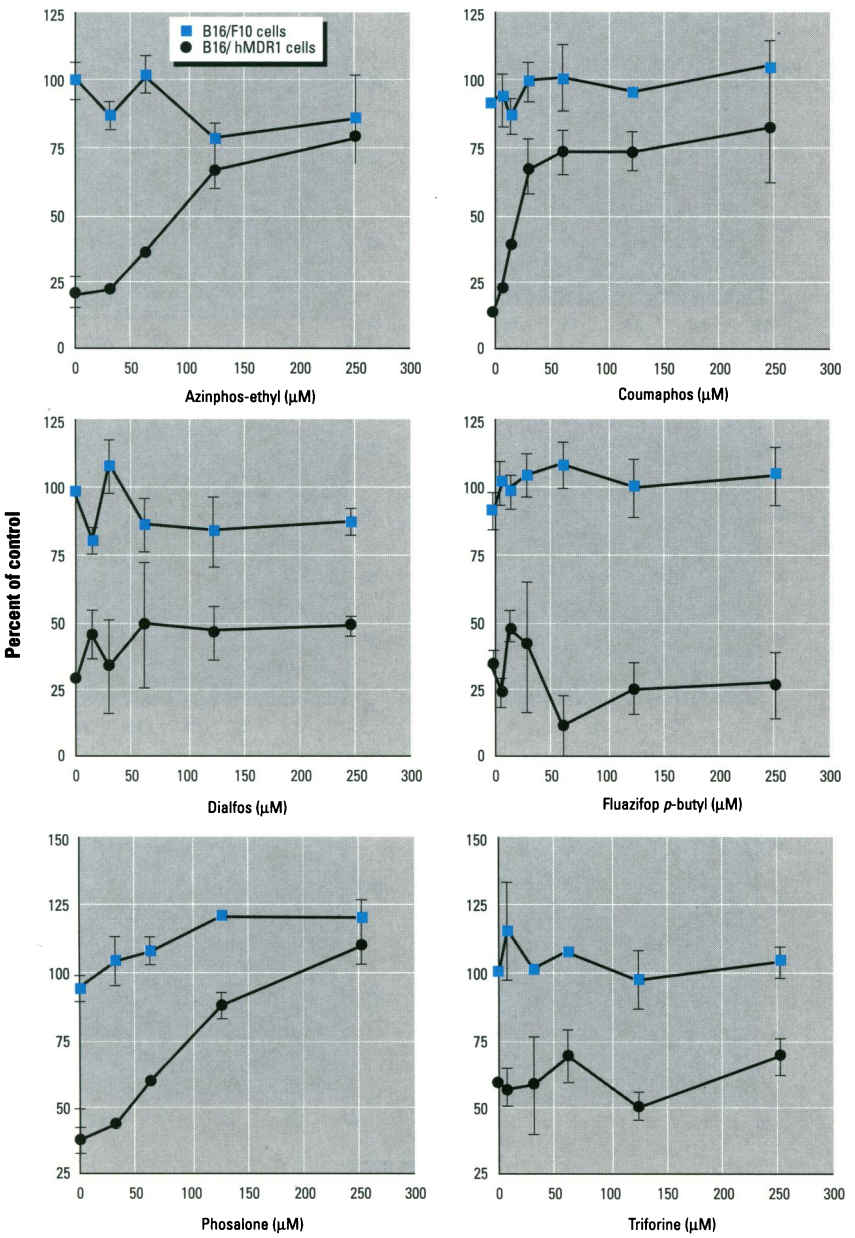

Figure 2. Inhibition of P-gp-mediated doxorubicin efflux by pesticides. B16/F10 cells and B16/hMDR1 cells were incubated for 4 hr in 50 μM doxorubicin along with increasing concentrations of the pesticides. The amount of doxorubicin accumulated in the cells was measured fluorimetrically and is presented as the percentage of the amount of doxorubicin measured in the positive control cells incubated in 10 μM verapamil. Values are the mean ± standard deviation of three replicates for each concentration of pesticide.

Table 4. Inhibitory potency of pesticides towards P-glycoprotein

Pesticide	EC_{50}[a] (CI)
Azinphos-ethyl	129 (115–143)
Coumaphos	26.9 (19.2–42.6)
Dialifos	>250
Fluazifop *p*-butyl	>250
Phosalone	96.4 (88.3–98.9)
Triforine	>250

Abbreviations: EC_{50}, median effective concentration; CI, 95% confidence interval.
[a]Values represent the concentration (μM) of each compound that increased the accumulation of doxorubicin in B16/hMDR1 cells to 50% of maximum as calculated by Spearman-Karber regression analysis. Results were derived from assays of at least six concentrations of each compound replicated three times.

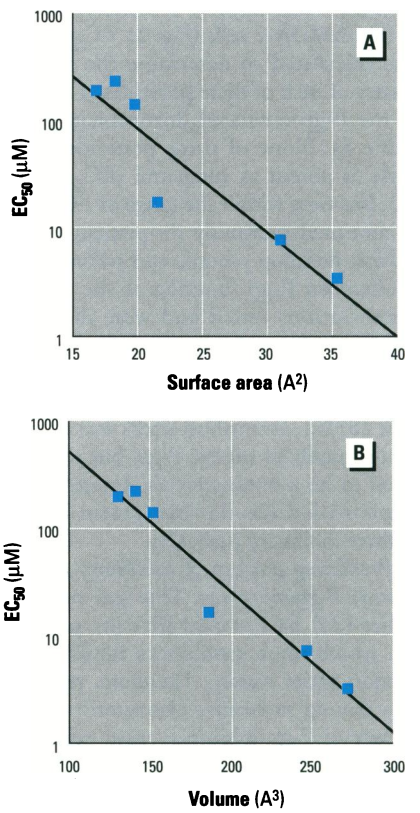

Figure 3. Correlation between P-gp inhibition potency and molecular surface area (A) or volume (B) of the pesticides. Potency is described by the effective concentration (EC_{50}) values as previously determined (*12*). Molecular surface area and volume of the pesticides are presented in Table 2.

Using the criteria defined in the tier 1 identification of P-gp transport substrates, the steroids cortisol and aldosterone meet the criteria for transport with respect to log K_{ow} and hydrogen-bonding potential, although both compounds have molecular weights that are slightly smaller than the 399 molecular weight requirement. Progesterone, on the other hand, is significantly smaller than the other steroids and does not meet the lipophilicity and hydrogen-bonding requirements for transport, and would be predicted to be an inhibitor of P-gp according to the tier 2 requirements. Cortisol and aldosterone have been shown experimentally to be transported by P-gp, while progesterone is not a transport substrate (*6*). Rather, progesterone has been shown experimentally to be a potent inhibitor of P-gp function (*28*). These observations further support the validity of the derived structure–activity relationships and suggest that additional analyses may reveal that compounds having a molecular weight of slightly less than 400 are also transport candidates. Interestingly, 400 is typically considered the approximate molecular weight limit above which chemicals are susceptible to biliary elimination (*29*). Perhaps P-gp and related transporters located on the canalicular membrane of hepatocytes are responsible for this size limitation.

The present study demonstrates that P-gp transport substrates have higher molecular weights, lower log K_{ow} values, and greater hydrogen-bonding potential than compounds that are not transport substrates. Further, the hydrogen-bonding potential of transport substrates is predominantly as hydrogen donors rather than hydrogen acceptors (data not shown). All of these characteristics are conferred to a molecule as a result of hydroxylation. Hydroxylation is a major biotransformation process leading to the elimination of many xenobiotics (*29*). Hydroxylation historically has been considered to facilitate xenobiotic elimination by increasing the aqueous solubility of the compound and thus mobilizing it in urine or bile. Present results suggest that hydroxylation may actually target xenobiotics for active elimination by P-gp. The example of the steroid hormones provided above lends support to this hypothesis in that both cortisol and aldosterone are hydroxylated derivatives of progesterone (*30*). Therefore, phase I hydroxylation enzymes may function in concert with phase III transport proteins to eliminate toxic compounds from cells and from the body. Precedents for similar interactions between biotransformation enzymes and active transport proteins exist. The multidrug resistance-associated protein (MRP) and the organic anion transporter (MOAT) are both involved in the cellular efflux of compounds following glucuronic acid or glutathione conjugation (*31,32*).

Transport substrates of P-gp tend to be hydrophilic, based upon calculated log K_{ow} values, while inhibitory ligands were relatively lipophilic. We noted previously that lipophilicity increased the ability of pesticides to inhibit P-gp up to a maximum potency at a log K_{ow} of 3.6–4.5 (*12*). Inhibitory potency progressively decreased as log K_{ow} values of pesticides increased beyond this optimum range. It is possible that compounds having a log K_{ow} of greater than 4.5 are so highly partitioned into cell membranes as to limit interaction with P-gp. It is currently not clear whether the P-gp inhibitors compete with transport substrates for the same binding site. Should these compounds interact at the same binding site, the present data suggests that increasing lipophilicity impedes transport while hydrogen bonding characteristics enhance transport potential.

Some inhibitors of P-gp had molecular weights that were somewhat lower than the minimum molecular weight of transport substrates, though potency of the inhibitors increased with increasing molecular volume or surface area. Assuming that the inhibitors competed for the same binding site as the transport substrates, the data indicates that compounds having a suboptimum molecular weight have the potential to bind to the transport site; binding affinity increases with increasing molecular mass, as indicated by molecular surface area or volume, but transport occurs only when a minimum molecular weight requirement is met.

The susceptibility of P-gp to inhibition by a variety of structurally diverse compounds implicates this protein as a possible target site of toxicity associated with many environmental chemicals. For example, a murine P-gp (*mdr2* gene product) has been implicated in the biliary elimination of phospholipids (*33*). Drugs including amitryptyline, chlorpromazine, promethazine, and propranolol have been shown to both inhibit P-gp function (*11*) and cause excess accumulation of phospholipids in tissues (*34*). Thus, inhibition of P-gp by some xenobiotics may result in phospholipid storage disorders. Disruption of another murine P-gp (*mdr1a* gene product) compromises the blood–brain barrier, resulting in increased accumulation of some xenobiotics in the brain (*7*). Accordingly, P-gp inhibitors may potentiate the toxicity of central nervous system toxicants. Continuous exposure to some xenobiotics results in decreased serum levels of corticosteroids (*35*). The inhibition of P-gp in the adrenal gland by the xenobiotics could be responsible for the reduced secretion of corticosteroid by this organ. Clearly, much is to be learned of the role of P-gp in the elimination of xenobiotics and as a target site for xenobiotic toxicity. An understanding of the characteristics that render xenobiotics as transport substrates or inhibitory ligands of P-gp will provide a foundation upon which additional experimental evidence can be generated to elucidate the role of this protein in chemical toxicity and elimination.

Table 5. Prediction of effective concentration (EC_{50}) for P-glycoprotein inhibition values using volume and surface area of inhibitory pesticides

Pesticide	Volume (A^3)	Predicted EC_{50} (μM)	Surface area (A^2)	Predicted EC_{50} (μM)	Measured EC_{50} (μM)
Azinphos-ethyl	167.1	56.7	21.2	60.6	128.9
Phosalone	171.6	49.6	21.8	53.8	96.4
Coumaphos	173.6	46.7	21.8	52.6	26.9

References

1. Gottesman MM, Currier S, Bruggemann E, Lelong I, Stein W, Pastan I. The multidrug transporter: mechanistic considerations. In: Cell Biology and Membrane Transport Processes, Vol 41 (Caplan M, ed). San Diego, CA:Academic Press, 1994;3–17.
2. Thiebaut F, Tsuruo T, Hamada H, Gottesman MM, Pastan I, Willingham MC. Cellular localization of the multidrug resistance gene product in normal human tissues. Proc Natl Acad Sci USA 84:7735–7738 (1987).
3. Horton JK, Thimmaiah KN, Houghton JA, Horowitz ME, Houghton PJ. Modulation by verapamil of vincristine pharmacokinetics and toxicity in mice bearing human tumor xenografts. Biochem Pharmacol 38:1727–1736 (1989).
4. van Kalken CK, Broxterman HJ, Pinedo HM, Feller N, Dekker H, Lankelma J, Giaccone G. Cortisol is transported by the multidrug resistance gene product P-glycoprotein. Br J Cancer 67:284–289 (1993).
5. Wolf DC, Horowitz SB. P-glycoprotein transports corticosterone and is photoaffinity-labeled by the steroid. Int J Cancer 52:141–146 (1992).
6. Ueda K, Okamura N, Hirai M, Tanigarwara Y, Saeki T, Kioka N, Komano T, Hori R. Human P-glycoprotein transports cortisol, aldosterone, and dexamethasone, but not progesterone. J Biol Chem 267:24248–24252 (1992).
7. Schinkel AH, Smit JJM, van Tellingen O, Beijnen JH, Wagenaar E, van Deemter L, Mol CAAM, van der Valk MA, Robanus-Maandag EC, te Riele HPJ. Disruption of the mouse *mdr1a* P-glycoprotein gene leads to a deficiency in the blood–brain barrier and to increased sensitivity to drugs. Cell 77:491–502 (1994).
8. Didier AD, Loor F. Decreased biotolerability for ivermectin and cyclosporin A in mice

exposed to potent P-glycoprotein inhibitors. Int J Cancer 63:263–267 (1995).
9. Lanning CL, Fine RL, Sachs CW, Rao US, Corcoran JJ, Abou-Donia MB. Chlorpyrifos oxon interacts with the mammalian multidrug resistance protein, P-glycoprotein. J Toxicol Environ Health 47:395–407 (1996).
10. Tew KD, Houghton PJ, Houghton JA. Preclinical and Clinical Modulation of Anticancer Drugs. Boca Raton, FL:CRC Press, 1993.
11. Hofsli E, Nissen-Meyer J. Reversal of multidrug resistance by lipophilic drugs. Cancer Res 50:3997–4002 (1990).
12. Bain LJ, LeBlanc GA. Interaction of structurally diverse pesticides with the human *MDR1* gene product P-glycoprotein. Toxicol Appl Pharmacol 141:288–298 (1996).
13. Bielder JL, Riehm H. Cellular resistance to actinomycin D in Chinese hamster cells *in vitro*; cross-resistance, radioautotrophic, and cytogenic studies. Cancer Res 30:106–110 (1970).
14. Christensen JG, LeBlanc GA. Reversal of multidrug resistance *in vivo* by oral administration of the phytochemical indole-3-carbinol. Cancer Res 56:574–581 (1996).
15. Zamora JM, Pearce HL, Beck WT. Physical–chemical properties shared by compounds that modulate multidrug resistance in human leukemia cells. Mol Pharmacol 33:454–462 (1988).
16. Tsuruo T, Ogawa M, eds. Drug Resistance as a Biochemical Target in Cancer Chemotherapy. San Diego, CA:Academic Press, 1992.
17. Kumar R. Simultaneous determination of some organophosphorus pesticides by high performance liquid chromatography. Biomed Chromatogr 3:272–273 (1989).
18. Rice LG. Rapid separation of pesticides by high-performance liquid chromatography with 3-μM columns. J Chromatogr 317:523–526 (1984).
19. Negre M, Gennari M, Cignetti A. High-performance liquid chromatographic determination of Fluazifop-butyl and Fluazifop in soil and water. J Chromatogr 387:541–545 (1987).
20. van Lancker MA, Bellemans LA, de Leenheer AP. Quantitative determination of low concentrations of adriamycin in plasma and cell cultures, using a volatile extraction buffer. J Chromatogr 374:415–420 (1986).
21. Debal V, Morjani H, Millot J-M, Angiboust J-F, Gourdier B, Manfait M. Determination of vinorelbine (Navelbine) in tumour cells by high-performance liquid chromatography. J Chromatogr 581:93–99 (1992).
22. Egorin MJ, Hildebrand RC, Cimino EF, Bachur NR. Cytofluorescence localization of adriamycin and daunorubicin. Cancer Res 40:2243–2245 (1974).
23. Hamilton MA, Russo RC, Thurston RV. Trimmed Spearman-Karber method for estimating median lethal concentrations in toxicity bioassays. Environ Sci Technol 11:714–719 (1978).
24. Tsuruo T, Iida H, Tsukagoshi S, Sakurai Y. Overcoming of vincristine resistance in P388 leukemia *in vivo* and *in vitro* through enhanced cytotoxicity of vincristine and vinblastine by verapamil. Cancer Res 41:1967–1972 (1981).
25. Gottesman MM, Patsan I. Biochemistry of multidrug resistance mediated by the multidrug transporter. Ann Rev Biochem 62:385–427 (1993).
26. Phang JM, Poore CM, Lopaczynska J, Yeh GC. Flavonol-stimulated efflux of 7,12-dimethylbenz(*a*)anthracene in multidrug-resistant breast cancer cells. Cancer Res 53:5977–5981 (1993).
27. Yeh GC, Lopaczynska J, Poore CM, Phang JM. A new functional role for P-glycoprotein: efflux pump for benzo[*a*]pyrene in human breast cancer MCF-7 cells. Cancer Res 52:6692–6695 (1992).
28. Ichikawa-Haraguchi M, Sumizawa T, Yoshimura A, Furukawa T, Hiramoto S, Sugita M, Akiyama S. Progesterone and its metabolites: the potent inhibitors of the transporting activity of P-glycoprotein in the adrenal gland. Biochim Biophys Acta 1158:201–208 (1993).
29. Hodgson E, Levi P. Introduction to Biochemical Toxicology. Norwalk, CT:Appleton & Lange, 1994.
30. Wilson JD, Foster DW. Textbook of Endocrinology. Philadelphia, PA:WB Saunders, 1985.
31. Oude Elferink RPJ, Jansen PLM. The role of the canalicular multispecific organic anion transporter in the disposal of endo- and xenobiotics. Pharmacol Ther 64:77–97 (1994).
32. Paul S, Breuninger LM, Kruh GD. ATP-dependent transport of lipophilic cytotoxic drugs by membrane vesicles prepared from MRP-overexpressing HL60/ADR cells. Biochemistry 35:14003–14011 (1996).
33. Smit JJM, Schinkel AH, Oude Elferink RPJ, Groen AK, Wagenaar E, van Deemter L, Mol CAAM, Ottenhoff R, van der Lugt NMT, van Roon MA. Homozygous disruption of the murine *mdr2* P-glycoprotein gene leads to a complete absence of phospholipid from bile and to liver disease. Cell 75:451–462 (1993).
34. Kodavanti UP, Mehendale HM. Cationic amphiphilic drugs and phospholipid storage disorder. Pharmacol Rev 42:327–353 (1990).
35. Hontela A. Endocrine and physicological responses of fish to xenobiotics: role of glucocorticosteroid hormones. Rev Toxicol (in press).